Field emission characteristics of the scanning tunneling microscope for nanolithography

T. M. Mayer, D. P. Adams, and B. M. Marder

Citation: Journal of Vacuum Science & Technology B **14**, 2438 (1996); doi: 10.1116/1.588751
View online: http://dx.doi.org/10.1116/1.588751
View Table of Contents: http://scitation.aip.org/content/avs/journal/jvstb/14/4?ver=pdfcov
Published by the AVS: Science & Technology of Materials, Interfaces, and Processing

Articles you may be interested in

Silicon metaloxidesemiconductor fieldeffect transistor with gate structures defined by scanned probe lithography
J. Vac. Sci. Technol. B **14**, 4153 (1996); 10.1116/1.588610

Three dimensional electron optical modeling of scanning tunneling microscope lithography in resists
J. Vac. Sci. Technol. B **14**, 4148 (1996); 10.1116/1.588609

Proximity effect correction for nanolithography
J. Vac. Sci. Technol. B **14**, 2445 (1996); 10.1116/1.588752

Lowvoltage electronbeam lithography with scanning tunneling microscopy in air: A new method for producing structures with high aspect ratios
J. Vac. Sci. Technol. B **14**, 1327 (1996); 10.1116/1.589090

Ambient scanning tunneling lithography of Langmuir–Blodgett and selfassembled monolayers
J. Vac. Sci. Technol. B **13**, 2837 (1995); 10.1116/1.588300

Redistribution subject to AVS license or copyright; see http://scitation.aip.org/termsconditions. Download to IP: 130.88.90.140 On: Thu, 15 Jan 2015 05:10:47

Field emission characteristics of the scanning tunneling microscope for nanolithography

T. M. Mayer,[a] D. P. Adams, and B. M. Marder
Sandia National Laboratories, Albuquerque, New Mexico 87185-1413

(Received 16 January 1996; accepted 29 May 1996)

We present a systematic study of the performance of scanning tunneling microscope (STM)-based, low energy electron beam lithography, using simulations of field emission from STM tips, emphasizing realistic conditions of tip geometry and operation. We calculate the potentials and electric field for a hemispherical model emitter in an axially symmetric system. Emission current density at the tip is calculated using the Fowler–Nordheim equation, and current density at the sample is obtained by calculating trajectories of emitted electrons. We characterize the beam diameter at the sample as a function of emitter radius, tip–sample bias, emission current, resist thickness, and tip work function. The beam diameter is primarily affected by the tip–sample gap, increasing at larger gaps, characteristic of high bias and large tip curvature. For optimal tip radius the beam diameter increases linearly with bias from approximately 2 nm at 5 V to 25 nm at 50 V. Beam diameter is nearly independent of emission current over the range 0.05–50 nA. Dielectric resist films cause an increase in beam diameter due to increased tip–substrate gap. Beam diameter is very sensitive to tip work function, increasing dramatically for low work function tips. Tips comprised of asperities on flat surfaces produce significantly smaller beams compared to ''standard'' tips of the same emitter radius. However, for low bias ($<$15 V) beam diameter becomes insensitive to tip geometry. We compare these simulations to selected experimental results to evaluate the limitations to performance and assess the feasibility of routine sub-10 nm structure fabrication using STM-based low energy electron beam lithography. © *1996 American Vacuum Society.*

I. INTRODUCTION

Low energy electron beam lithography is an attractive option for nanometer-scale device fabrication because of the virtual elimination of scattering effects which limit resolution in conventional electron beam lithography.[1,2] The scanning tunneling microscope (STM) operating in field emission mode is widely employed to produce electron beams with energy $<$100 eV for this purpose. The relative simplicity of the system, small beam size, and very high current density at low energy makes the STM an ideal research tool, and a potentially useful manufacturing tool for nanometer-scale structures.

There are a number of possible approaches to nanostructure fabrication using the STM,[3,4] but the most promising for widespread utility is low energy electron exposure of an imaging material (resist), which is used to transfer a pattern into a substrate or film. A variety of resist materials has been investigated using STM-based lithography, including PMMA and other conventional resists,[2,5,6] thin siloxane films,[7] molecular films such as Langmuir–Blodgett and self-assembled monolayer films,[8–10] thin inorganic materials, such as CaF_2,[11] and adsorbed atomic layers, particularly hydrogen on Si.[12–14]

The limitations to feature size and resolution obtainable by this process are functions of both the resist material performance and the ability to form a small diameter beam of low energy electrons. However, there have been few investigations of the performance of a STM tip as a low energy electron beam source. McCord and Pease[15] performed simulations of electron emission from an isolated sphere in the field emission regime (5 eV$<E<$100 eV), and identified many of the major features of STM-based lithography. Beam diameter at the sample was shown to be a sensitive function of the tip radius, gap, and tip–sample bias.

Since this early modeling effort, many experimental demonstrations of nanometer-scale lithography have appeared. In particular, we have shown that it is possible to directly measure the current distribution from STM tips used in lithographic processes.[14] These results give impetus to more extensive modeling using realistic emitter structures and operating conditions that may be compared directly to experiments. In this article we present results of field emission simulations of STM tips as low energy ($<$50 eV) electron beam sources for nanolithography. We emphasize comparison to realistic conditions where a tip is operated in constant voltage and current mode, using feedback control of the gap to maintain a fixed current. We investigate the effects of bias voltage and tip radius on beam diameter for idealized hemispherical tips. We also investigate the dependence of beam diameter on total emission current, tip work function, and the presence of a dielectric (resist) layer between the tip and substrate. Alternate tip configurations in which the electric field at the tip is tailored to confine the trajectories of emitted electrons into a small beam diameter are evaluated. These results help establish reasonable expectations for performance of STM-based nanolithography.

Finally, we critically examine selected experimental systems to evaluate their performance compared to the expected

[a]Electronic mail: tmmayer@sandia.gov

Redistribution subject to AVS license or copyright; see http://scitation.aip.org/termsconditions. Download to IP: 130.88.90.140 On: Thu, 15 Jan 2015 05:10:47

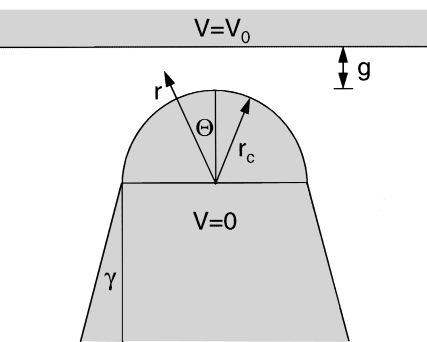

FIG. 1. Geometry of the field emission calculation. The cathode (tip) and anode (sample) are assumed to be conducting.

emitter characteristics. We conclude that routine sub-10 nm lithography is feasible using low energy (<20 V) exposures and very thin, atomic or molecular layer resists.

II. FIELD EMISSION SIMULATIONS

The field emission simulations are carried out in the geometry shown in Fig. 1. We define an axially symmetric system, in which the cathode (emitter) is a conducting hemisphere of radius r_c. The emitter is attached to a shank with a variable cone angle, γ. The anode (sample) forms a conducting plane at some distance z_a, where the gap between emitter and sample is $g=(z_a-r_c)$. A dielectric film (resist) can be interposed between the tip and sample.

The potential in the space between the anode and cathode obeys Laplace's equation:

$$\nabla \epsilon \nabla V=0, \tag{1}$$

where V is the potential at any point in the vacuum or resist film and ϵ is the dielectric constant of the medium. In spherical polar coordinates Eq. (1) is[16]

$$\frac{\partial}{\partial r}\epsilon r^2\frac{\partial V}{\partial r}+\frac{1}{\sin\,\theta}\frac{\partial}{\partial \theta}\epsilon\,\sin\,\theta\frac{\partial V}{\partial \theta}=0. \tag{2}$$

After specifying the emitter geometry and the emitter–sample gap, we define a set of grid points in r and θ, and solve Eq. (2) for $V(r,\theta)$ using a finite difference method with the boundary conditions that $V=0$ at the cathode (tip) and $V=V_0$ at the anode (sample).

The emission current density at the tip is given by the Fowler–Nordheim equation:[17]

$$J=\frac{AE^2}{\phi}\exp\left(\frac{B}{\phi^{1/2}}-\frac{C\phi^{3/2}}{E}\right), \tag{3}$$

where E is the electric field, ϕ is the work function of the tip, and A, B, and C are constants. The electric field at the emitter surface is the gradient of $V(r_c,\theta)$. We integrate the emission over the entire tip surface and adjust the anode distance, z_a, to obtain the desired total emission current at a fixed bias.

Sample current density is obtained by calculating trajectories of electrons leaving the tip at different angles, and mapping the emission current density from the tip to the sample. We assume that electrons leave the tip normal to its surface, with zero kinetic energy, and we ignore scattering of the electrons in the resist film (if present).

Most calculations are carried out using a tip work function, ϕ=4.5 eV, appropriate for a W tip.[18] The shank angle, γ, has minimal effect on the electric field at the tip and the trajectories of electrons traveling to the sample, except for very sharp tips and large tip–sample distances. All "standard" tip simulations are carried out using a shank angle of 20°. We also explore some alternate tip geometries in an attempt to confine or focus the electron current at the sample by tailoring the electric field in the vicinity of the tip.

III. RESULTS AND DISCUSSION

A. Characteristics of standard tips

We have examined emission characteristics of standard tips as a function of tip radius, anode voltage, total emission current, resist thickness, and tip work function. In typical operation of an STM-based lithography system, the anode voltage and emission current are held constant, and the gap is adjusted by a feedback circuit to maintain constant electric field at the tip and thus constant emission. This is a very important aspect, since the electric field configuration in the gap and trajectories of electrons to the sample are very sensitive to the tip–sample gap. For direct comparison to this mode of STM operation, all simulations presented here treat the gap as a free parameter. We have previously shown that these simulations agree well with the gap measured as a function of anode voltage in an operating STM.[14] Since we are primarily interested in the current density distribution at the sample, results are presented in terms of the beam diameter at the sample surface. We define the beam diameter as that which contains 60% of the total current. (This is approximately equivalent to the standard method of measuring beam diameter in electron beam lithography systems.)

Considering standard tips with radii of 5–50 nm, we calculate the beam current density distributions for biases from 5 to 50 V. The current density distribution at the sample follows a functional form of approximately $\exp(-r^{1.8}/\alpha)$, where the width parameter, α, depends on the bias and the tip–sample gap. The beam diameter as a function of bias voltage is shown in Fig. 2(a). The increase in beam diameter with increasing bias, for all tip radii, is primarily due to increased gap at increased bias, and resulting radial spreading of electron trajectories. This is demonstrated in Fig. 2(b), where the beam diameter is seen to increase approximately linearly with the gap that is required to produce 1 nA current at the given bias.

Tips with higher curvature (small r_c) develop higher electric fields at a given V_0 and gap, so that the feedback circuit responds by retracting the tip to maintain the preset emission. For sharper tips emission also occurs over a larger range of angle, θ, at the apex of the tip. This results in the phenomenon shown in Fig. 2(a) in which sharp tips give smaller beam diameters at low bias but larger beam diameters at increasing bias, due to the larger gap. These results are in good agreement with the earlier simulations of Mc-

Redistribution subject to AVS license or copyright; see http://scitation.aip.org/termsconditions. Download to IP: 130.88.90.140 On: Thu, 15 Jan 2015 05:10:47

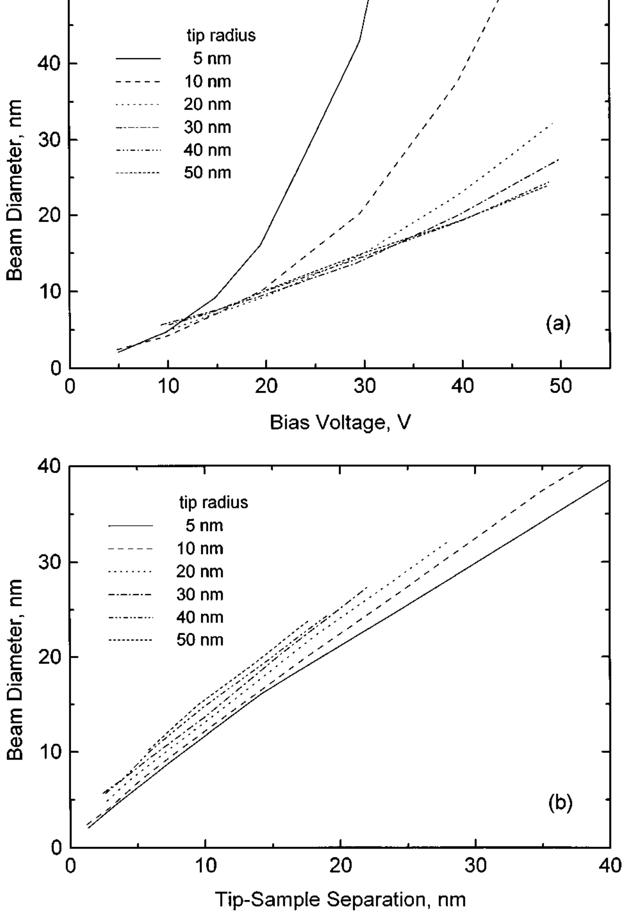

FIG. 2. (a) Beam diameter vs sample bias for various tip radii at 1 nA emission current; (b) beam diameter vs tip sample separation for the calculations shown in (a).

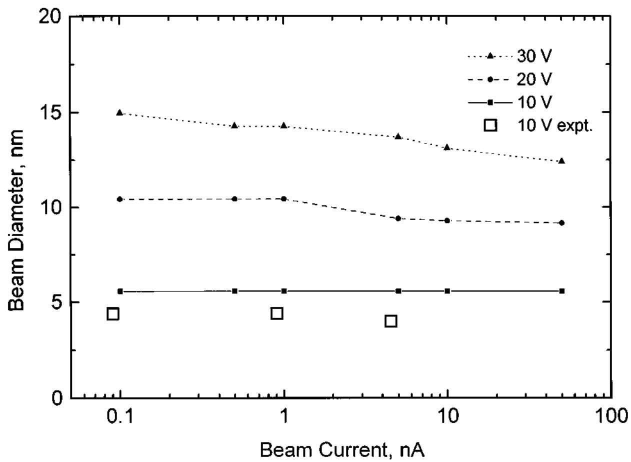

FIG. 3. Beam diameter vs emission current for a 30-nm-radius tip at 10–30 V sample bias. Experimental data (from Ref. 14) are for 10 V bias.

Cord and Pease,[15] who demonstrated that there is an optimum ratio of tip radius to gap which gives minimum beam diameter. In general, the beam diameter increases approximately linearly with bias for optimum tip radius, and best performance is achieved at low bias for all tip radii.

We have examined other influences on beam diameter for the standard tip geometry. Dependence of beam diameter on beam current is shown in Fig. 3, for a tip radius of 30 nm, and for several biases. The beam diameter decreases slightly at high current due the decreased gap required for higher fields. But the dependence is fairly weak over three orders of magnitude of current due to the steep dependence of emission on electric field characteristic of the Fowler–Nordheim emission process. Only very small changes in gap are necessary to alter the field sufficiently for large variations in current. We have ignored space charge effects, which can substantially alter the trajectories of low energy electrons in high current density beams. For currents <1 μA, at typical bias and tip–sample gap, there is, on average, only one electron in the gap at a time.

The presence of a resist film will alter the electric field at the tip and in the gap. The primary effect of interposing a resist film will be to increase the tip–sample separation, causing increased beam diameter. A resist will also have a higher dielectric constant than vacuum (or air). Presuming that the tip is not allowed to penetrate the resist film, the electric field in the vacuum gap will be approximately $E(\text{gap}) \approx \epsilon E(\text{resist})$, where ϵ is the resist dielectric constant. Because $E(\text{resist})$ decreases with increasing resist thickness, $d(\text{gap})$ must decrease in order to produce adequate electric field at the tip to maintain emission. For thick resists, the tip must be very close to the resist surface in order to maintain emission [$d(\text{gap})<1$ nm for resist thickness of 50 nm]. In general, particularly for resists with low dielectric constant, as resist thickness increases, it is difficult to maintain an adequate electric field at the tip to provide the desired emission current. The tip will then be forced to penetrate the resist in order to establish the required electric field.

Beam diameter at the resist/vacuum interface is small, because of the reduced $d(\text{gap})$, however the beam spreads traversing the resist film. Calculations for a tip radius of 30 nm, 20 V bias, and $\epsilon=3$ show that the beam diameter at the resist/substrate interface increases with resist thickness with a slope of ≈ 0.3. For this calculation, we assume the electron travels through the resist film without scattering. Of course electrons will scatter in the resist, as they must to deposit energy, and the volume of exposed material will be further increased by the scattering of these low energy electrons, comparable to the scattering of secondary electrons produced by high energy electron beam exposure.

Alternate tip materials with lower work function or tips with low work function adsorbates[19] can be employed. This leads to higher emission current at a given electric field, as seen from Eq. (3). This is generally desirable for other field emission devices, such as emitters for electron microscopes, vacuum microelectronics, or display devices. However in a lithographic application, a low work function tip will achieve a given current density at a larger tip–sample gap, resulting in larger beam diameter at a given current and voltage than for the same geometry tip of a higher work function. The effect is quite dramatic, and is shown in Fig. 4. Plotted are

Redistribution subject to AVS license or copyright; see http://scitation.aip.org/termsconditions. Download to IP: 130.88.90.140 On: Thu, 15 Jan 2015 05:10:47

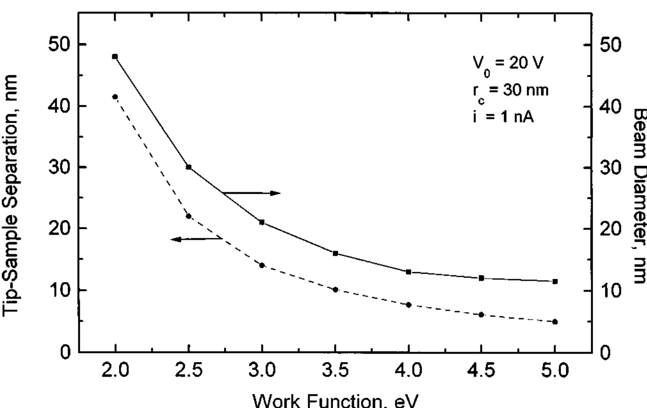

FIG. 4. Effect of tip work function on tip–sample separation and beam diameter for a 30-nm-radius tip, 20 V bias, and 1 nA emission.

tip–sample gap and beam diameter at the sample as a function of tip work function for a 30-nm-radius tip at 20 V bias and 1 nA current. The direct correlation of tip–sample gap and beam diameter is well demonstrated here. Additional effects of tip geometry and bias behave in a similar manner to Fig. 2.

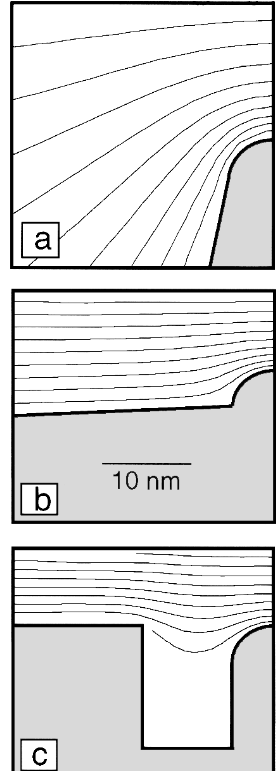

FIG. 5. Equipotential contours for (a) standard tip, (b) asperity tip, and (c) recessed tip. Contour interval is $0.1V_0$. Tip–sample gap is that required for 1 nA emission at 20 V bias.

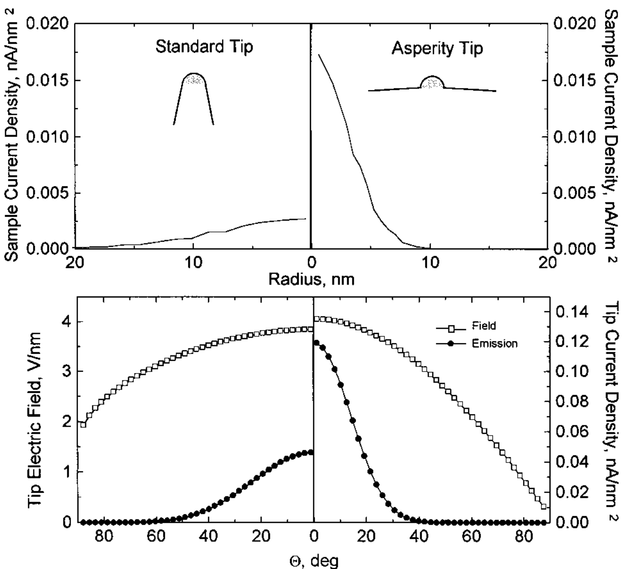

FIG. 6. Tip electric field, tip emission current density, and sample current density for standard and super tips. Emitter radius is 5 nm, bias is 20 V, and emission is 1 nA for each.

B. Alternate tip configurations

The idealized standard tip configuration shown in Fig. 1 is unlikely to be representative of real electron emitters for a number of reasons. While tips may appear round and smooth on a macroscopic scale, invariably, microscopic details of the tip surface will include local asperities due to tip preparation, tip alternation, contamination, or even discontinuities due to atomic steps and defects on the surface. These will all lead to a local alteration of the electric field and emission characteristics that deviate from the ideal spherical tip.[20] It is generally assumed in scanning tunneling microscopy that tunneling occurs primarily through only a few atoms at a local asperity, and many tip preparation procedures are effectively intended to produce small asperities.

Asperities can also be intentionally fabricated in a controlled fashion to produce a desired electric field configuration at the tip. "Super tips"[21,22] have been constructed by producing controlled asperities on the end of relatively blunt tips for use as electron and ion emitters with a reduced angular emission profile. While a very small asperity indicates a high curvature emitter, the electric field is suppressed at large polar angles by the proximity of a flat surface, and emission is restricted to a small range of polar angles at the apex of the asperity. The result is a beam that is focused in the forward direction.

This focusing effect can also be useful in lithographic applications. We have examined to alternate tip configurations intended to produce this focusing effect, shown in Fig. 5 along with equipotential contours for a tip–sample gap that would produce 1 nA current at a sample bias of 20 V. The origin of the effect is clear from the shapes of the equipotential contours and the recognition that field lines are perpendicular to the potential contours. The standard tip in Fig. 5(a)

Redistribution subject to AVS license or copyright; see http://scitation.aip.org/termsconditions. Download to IP: 130.88.90.140 On: Thu, 15 Jan 2015 05:10:47

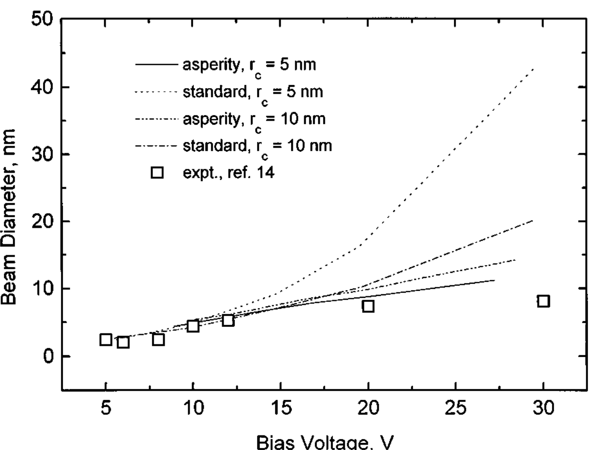

FIG. 7. Beam diameter vs sample bias for standard and asperity tips with radii of 5 and 10 nm at 1 nA emission. Experimental data are from Ref. 14.

with a 5 nm radius exhibits large curvature of the potential contours, leading to a large degree of radial spreading of the electron trajectories. Figure 5(b) depicts an asperity tip consisting of a hemisphere with 5 nm radius on a nearly flat surface (shank angle =85°). The potential contours are comparatively much flatter in the region of the emitter, giving electron trajectories focused in the forward direction. Figure 6 shows a comparison of the electric field and emission profiles at the tip and the current profile at the surface for the standard tip and the asperity tip in Figs. 5(a) and 5(b). For the standard tip, at 20 V bias and 1 nA emission, the tip–sample gap is 17 nm, and emission occurs out to >40° polar angle on the tip. This results in a diffuse beam with a diameter of 21 nm. The asperity tip, however, shows high field and significant emission only out to 30° polar angle, and the tip–sample gap is reduced to 10 nm. This gives a beam diameter of 9 nm, or less than half that of the standard tip.

Beam diameter versus sample bias for asperity tips and standard tips of 5 and 10 nm tip radius are shown in Fig. 7. The characteristics of the asperity tip emission follow the same trends as those for the standard tip, only with decreased beam diameter due to the focusing effect and reduced tip–sample separation. We note from Fig. 7 that the effect is most pronounced for small asperities. For the larger (10 nm) asperity the alteration of the potential near the tip apex is less pronounced and the focusing effect is minimized. We also note that the focusing effect is most pronounced at higher bias, where the tip–sample separation is large. Small tip–sample separation at low bias also results in a minimal alteration of the potential near the apex, and minimal focusing.

Comparison of Fig. 7 with Fig. 2(a) shows that the 5 nm asperity tip produces a beam slightly smaller than the "optimum" standard tip at all biases above 15 V. However, at biases of less than about 15 V, the beam diameter is relatively insensitive to the tip geometry, whether it is an asperity or standard tip. This insensitivity suggests that for low voltage lithography one need not be very concerned about the nature of the tip.

Further focusing of electron trajectories can be obtained using an emitter structure similar to that shown in Fig. 5(c). This is a recessed emitter than could potentially be fabricated by ion sputtering techniques similar to those used to make extremely sharp tips for metrology applications,[23] and recessed emitters for vacuum microelectronics.[24,25] In this schematic example the recessed tip is a hemisphere with a diameter of 5 nm. The top of the tip is at the same height as the planar cathode, and the tip is separated from the rest of the cathode by a 10-nm-wide trench. The intention here is to use the planar cathode as a Wehnelt cylinder to focus electron trajectories in the forward direction. The focusing effect is evident, producing a beam diameter of 7.2 nm for the conditions of Fig. 6, compared to 18 nm for the standard tip and 8.8 nm for the asperity tip. The performance of this tip depends primarily on the width of the trench between the tip and the planar cathode. Structures with trench width of >20 nm perform less well than the tip of Fig. 5(b). Performance could be increased by narrowing the trench or by recessing the emitter below the surface of the planar cathode. Of course the corners of the planar cathode would have to be suitably rounded to prevent development of an excessive field at this corner. Fabrication of such a tip becomes problematic, and operation of a recessed tip in close proximity to a sample may result in the planar cathode being too close to the sample (with very high electric field at the planar cathode surface). This type of emitter structure may be useful in other field emission devices that require a focused electron beam.[26]

We have not attempted to model emitters consisting of only a single or very few atoms. Such ultrasharp tips have been fabricated and used as point source emitters for electron microscopes.[19,27] As expected, they demonstrate very high fields and emission current densities at the apex. Cutler and co-workers,[28] however, have shown that ultrasharp tips do not obey the usual formulation of the Fowler–Nordheim emission theory, and suggest that Eq. (3) may be in error by orders of magnitude for tip radii <10 nm. It appears that a more sophisticated treatment of the field emission process is required for modeling atomically sharp tips.

C. Comparison to experiments

While most experimental demonstrations of STM-based lithography have not specified tip geometry nor directly measured electron current distributions, we can compare these simulations to a number of experimental results demonstrating feature sizes on the order of 10 nm that have appeared over the past few years.

We have directly measured the electron current distribution at the sample by imaging the distribution of desorbed H atoms from Si(001) surfaces in the STM, reported elsewhere.[14] Above a threshold energy of 6–8 eV, this electron stimulated desorption process provides a direct measure of the electron flux distribution with minimal electron scattering effects. We also measured the tip–sample separation as a function of sample bias. All of these measurements were made with a W tip, prepared by electrochemical etching, that was not evaluated prior to introduction into the STM. Over the range of 5–30 V bias, we observed a beam diameter that

Redistribution subject to AVS license or copyright; see http://scitation.aip.org/termsconditions. Download to IP: 130.88.90.140 On: Thu, 15 Jan 2015 05:10:47

varied from 2 to 8 nm. The measured tip–sample gap ranged from, nominally, 1 nm at tunneling conditions of 2 V bias to 16 nm at 40 V. The tip–sample gap agrees well with standard tip simulations for hemispherical emitters with $r=30–50$ nm.

The observed beam diameters, however, were smaller than those calculated for standard tips of optimum radius, particularly at higher bias, but agree well with the simulations including focusing effects associated with emission from asperities on a blunt tip, shown in Fig. 7. We do not know if emission is occurring from a single site or from a number of asperities. (We have seen experimental evidence for multiple site emission, on occasion.) Beam diameter was observed to be essentially constant over more than two orders of magnitude of emission current at fixed bias, in good agreement with the calculations, as shown in Fig. 4. The estimated functional form of the beam profile is also in reasonable agreement with the calculations. The experimental data are best fit with an exponential form, decaying radially as r^1 to $r^{1.5}$, while the calculations indicate an $r^{1.8}$ dependence. Feature sizes produced as a function of exposure dose show broadening, consistent with the beam profile measured at low dose, with some evidence of electron reflection effects at high bias and dose. This system, by eliminating scattering effects and using an ideally thin, self-developing resist appears limited only by electron current distribution from the tip.

Effects of electron scattering, large tip–sample separation with thick resists, and postexposure processing can all limit the size of features that can be fabricated independently of the performance of a given tip. Exposure of self-assembled monolayer resists should show minimal electron scattering effects and minimal beam spreading due to increased tip–sample gap, and most accurately reflect the beam diameter at the surface. Marrian *et al.*[10] have exposed monolayers of a phenylethylenediaminemethoxysilane resist, approximately, 1 nm thick and achieved linewidths of <10 nm for low voltage (<10 V) exposures. Exposures of 4-chloromethylphenyltrichlorosilane at 8 V produced features <20 nm (measurement limited by the grain size of the Ni subsequently plated on the sample). Direct comparison to our simulations is not possible, but these studies appear to be approaching the limit of patterning ability determined by beam diameter.

Zhang *et al.*[8] have examined polymethylmethacrylate (PMMA) and polyvinylcinnamate films prepared by the Langmuir–Blodgett technique that give 4.5–14-nm-thick films. Linewidths of 30–100 nm were observed after exposure at 20–30 V sample bias, and various development and pattern transfer procedures. These dimensions are considerably larger than the expected beam diameter at these conditions and probably reflect the effects of resist development and subsequent etching processes on broadening of the feature dimension.

A number of investigators have examined thicker films of conventional electron beam resists prepared by spin-on techniques. McCord and Pease[5] report fabrication of 20 nm linewidths in 20-nm-thick films of PMMA. Dobisz and Marrian[2] and Marian *et al.*[6] report linewidths from 30 to 50 nm for 50–80-nm-thick resist (Shipley SAL-601) films. These results apparently show little broadening due to resist processing and are consistent with broadening of the electron beam profile by the presence of a thick resist film.

While a number of studies appear to be approaching the beam-limited performance, definition of sub-10 nm features has only been demonstrated for atomic or molecular layer resists. As suggested by the simulations, beam spreading (and ultimately electron scattering) in thicker (>10 nm) resist films leads to larger feature sizes. Routine sub-10 nm lithography may be limited to very thin resists, such as self-assembled monolayer films, or the adsorbed atomic or molecular layer.

IV. SUMMARY

We have presented a systematic study of the performance of STM-based, low energy electron beam lithography based on simulations of field emission from STM tips in close proximity to a substrate surface. The major factor in determining the beam diameter is the tip–sample gap, which is set to obtain the necessary field strength at the tip for the desired emission. The beam diameter increases as a function of bias because of the larger gap at higher voltage and subsequent spreading of the electron trajectories. At a given bias there is a trade-off between tip radius and tip–sample gap that leads to an optimum tip radius for minimum beam size. At low bias (<10 V) sharp tips give smallest beam size, whereas at high bias (>40 V) more blunt tips result in smaller beam diameter. For optimal tip radius the beam diameter increases linearly with bias from approximately 2 nm at 5 V to 25 nm at 50 V. Beam diameter is nearly independent of emission current over the range 0.05–50 nA.

Dielectric resist films interposed between tip and sample cause an increase in beam diameter due to increased tip–substrate gap. Reduction of the tip work function results in a dramatic increase in beam diameter due to the larger gap required to obtain the desired emission from a low work function tip.

We have examined alternative tip structures intended to tailor the electric field in the vicinity of the tip and focus the electron beam to a smaller diameter. Asperities consisting of a small radius hemisphere on a nearly flat surface produce beams with significantly smaller diameter than those produced by a standard tip of the same emitter radius. However, for sample bias <15 V the beam diameter becomes relatively insensitive to tip geometry, converging on a beam diameter of ~5 nm at 10 V bias for all tips.

The simulations agree quite well with experiments that directly measure the current distribution at the sample. These results, using adsorbed atomic H as a resist, display feature sizes limited only by the characteristics of the electron emitter. Experiments using molecular layer resists, such as self-assembled monolayer films, also approach resolution limits set by the electron beam diameter. Given the results of the simulations presented here and the beam-diameter-limited

Redistribution subject to AVS license or copyright; see http://scitation.aip.org/termsconditions. Download to IP: 130.88.90.140 On: Thu, 15 Jan 2015 05:10:47

performance of a number of experimental systems, we feel confidence that routine sub-10 nm structure fabrication using STM-based low energy electron beam lithography is feasible with current techniques.

ACKNOWLEDGMENTS

The authors have enjoyed fruitful discussions with B. S. Swartzentruber, G. L. Kellogg, and H. Koops. This work was supported by the U.S. Department of Energy under Contract No. De-AC04-94AL850000.

[1]Y. W. Yau, R. F. W. Pease, A. A. Iranamesh, and K. J. Polasko, J. Vac. Sci. Technol. **19**, 1048 (1981).
[2]E. A. Dobisz and C. R. K. Marrian, J. Vac. Sci. Technol. B **9**, 3024 (1991).
[3]G. M. Shedd and P. M. Russell, Nanotechnology **1**, 67 (1990).
[4]*Technology of Proximal Probe Lithography*, edited by C. R. K. Marrian (SPIE Institutes for Advanced Optical Technologies, Bellingham, WA, 1993), Vol. IS10.
[5]M. A. McCord and R. F. W. Pease, J. Vac. Sci. Technol. B **4**, 86 (1986).
[6]C. R. K. Marrian, E. Dobisz, and J. A. Dagata, J. Vac. Sci. Technol. B **10**, 2877 (1992).
[7]S. W. Park, H. T. Soh, C. F. Quate, and S. I. Park, Appl. Phys. Lett. **67**, 2415 (1995).
[8]H. Zhang, L. S. Hordon, S. W. J. Kuan, P. Maccagno, and R. F. W. Pease, J. Vac. Sci. Technol. B **7**, 1717 (1989).
[9]L. Stockman, G. Neuttiens, C. van Haesendonck, and Y. Bruynsereade, Appl. Phys. Lett. **62**, 2935 (1993).
[10]C. R. K. Marrian, F. K. Perkins, S. L. Brandow, T. S. Koloski, E. A. Dobisz, and J. M. Calvert, Appl. Phys. Lett. **64**, 390 (1994); F. K. Perkins, E. A. Dobisz, C. R. K. Marrian, and S. L. Brandow, J. Vac. Sci. Technol. B **13**, 2841 (1995).
[11]M. A. McCord and R. F. W. Pease, J. Vac. Sci. Technol. B **5**, 430 (1987).
[12]R. S. Becker, G. S. Higashi, Y. J. Chabal, and A. J. Becker, Phys. Rev. Lett. **65**, 1917 (1990).
[13]J. W. Lyding, G. C. Abeln, T. C. Shen, C. Wang, and J. R. Tucker, J. Vac. Sci. Technol. B **12**, 3735 (1994).
[14]D. P. Adams, T. M. Mayer, and B. S. Swartzentruber, J. Vac. Sci. Technol. B **14**, 1642 (1996).
[15]M. A. McCord and R. F. W. Pease, J. Vac. Sci. Technol. B **3**, 198 (1985).
[16]P. L. Lorrain, D. P. Corson, and F. Lorrain, *Electromagnetic Fields and Waves* (Freeman, New York, 1988).
[17]R. H. Fowler and L. W. Nordheim, Proc. R. Soc. London Ser. A **119**, 173 (1928); C. A. Spindt, I. Brodie, L. Humphrey, and E. R. Westerberg, J. Appl. Phys. **47**, 5248 (1976).
[18]H. B. Michaelson, J. Appl. Phys. **48**, 4731 (1977).
[19]R. Morin and H.-W. Fink, Appl. Phys. Lett. **65**, 2362 (1994).
[20]R. Gomer, *Field Emission and Field Ionization* (Harvard University Press, Cambridge, 1961).
[21]K. Jousten, K. Bohringer, R. Borret, and S. Kalbitzer, Ultramicroscopy **26**, 301 (1988).
[22]R. Borret, K. Bohringer, and S. Kalbitzer, J. Phys. D: Appl. Phys. **23**, 1271 (1990).
[23]M. J. Vasile, D. A. Grigg, J. E. Griffith, E. A. Fitzgerald, and P. E. Russell, Rev. Sci. Instrum. **62**, 2167 (1991).
[24]J. Ishikawa, T. Ohtake, Y. Goto, H. Tsuji, N. Fukuyama, K. Inoue, S. Nagamachi, Y. Yamakage, M. Ueda, H. Maruno, and M. Asari, J. Vac. Sci. Technol. B **13**, 452 (1995).
[25]W. K. Lo, M. Skvarla, C. W. Lo, H. G. Craighead, and M. S. Isaacson, J. Vac. Sci. Technol. B **13**, 2441 (1995).
[26]M. G. R. Thompson, J. Vac. Sci. Technol. B **13**, 2455 (1995).
[27]H.-W. Fink, IBM J. Res. Devel. **30**, 460 (1986); H.-W. Fink, Phys. Scr. **38**, 260 (1988).
[28]P. H. Cutler, J. He, N. M. Miskovsky, T. E. Sullivan, and B. Weiss, Prog. Surf. Sci. **42**, 169 (1993).

Redistribution subject to AVS license or copyright; see http://scitation.aip.org/termsconditions. Download to IP: 130.88.90.140 On: Thu, 15 Jan 2015 05:10:47